Article

An isoquinolin-1(2H)-imine derivative induces cell death via generation of reactive oxygen species and activation of JNK in human A549 cancer cells[†]

Jing Liu[1#], Tongyang Liu[1#], Hanchuan Mou[1], Shuting Jia[1], Chao Huang[2], Shengjiao Yan[2], Jun Lin[2*], Ying Luo[1*], Jihong zhang[1*]

[1] Laboratory of Molecular Genetics of Aging and Tumor, Faculty of Medicine，Kunming University of Science and Technology, Kunming 650500, P.R. China

[2] Key Laboratory of Medicinal Chemistry for Natural Resource, Ministry Education, School of Chemical Science and Technology, Yunnan University, Kunming, 650091, P.R. China

[*] Correspondence to Jihong Zhang, email zhjihong2000@126.com. Lab of Molecular Genetics of Aging and Tumor, Faculty of Medicine, Kunming University of Science and Technology, 727 Jing Ming Nan Road, Chenggong County, Kunming 650500, Yunnan Province, China.

Telephone: 0086-871-65920753

Fax: 0086-871-65920753

[#] The authors contribute to the paper equally

Abstract

Background: Compound 11-benzoyl-10-chloro-7,9-difluoro-6-imino-2,3,4,6-tetrahydro-1H-pyrimido[1,2-b]isoquinoline-8-carbonitrile (HC6h) is a novel polyhalo 1,3-diazaheterocycle fused isoquinolin-1(2H)-imines derivative, which displays good anticancer activity and low toxicity in vivo. However, the underlying anticancer mechanisms have not previously been identified.

Methods: The proliferation of A549 was assessed by MTT assay. The reactive oxygen species (ROS) level was assessed in A549 with a H_2DCFDA probe. Mitochondrial membrane potential was measured using the JC-1 staining. Apoptosis were measured by annexin-V/PI assay and autophagy by acridine orange staining and GFP-LC3 fluorescence assay. The expression of autophagic and apoptotic proteins was determined by Western blot.

Results: The compound HC6h increased accumulation of vesicles, acridine orange-stained cells and LC3-II in A549 cells. Inhibition of compound HC6h-induced autophagy by bafilomycin A1 increased apoptosis. Compound HC6h enhanced activation of caspase-3, caspase-9 and PARP cleavage in A549 cells. Compound HC6h leads to the rapid generation of intracellular ROS. Moreover, compound HC6h induced phosphorylation of JNK and was conferred by the increased ROS levels. Furthermore, down-regulation of JNK attenuated autophagic and apoptotic effect in response to HC6h.

Conclusion: The induction of ROS upon HC6h treatment leads to the activation of JNK that mediates autophagy and apoptosis in human A549 cancer cells. This article is protected by copyright. All rights reserved

Key words: isoquinolin; autophagy; apoptosis; ROS

Introduction

Lung cancer is the most common cancer in both women and men, and also the leading cause of cancer death. Although multiple diagnostic procedures and therapeutic options are developed recently, the overall outlook has not greatly improved for most patients，with the overall 5-year survival having only slightly increased over the last decade from 15.7% to 17.4%. It is well known that resisting cell death is a hallmark of cancer which contributes to tumor progress and resistance to conventional anti-tumor therapies [1]. Therefore, targeting cancer cell death pathways is an efficient strategy to kill cancer.

Cell death includes apoptosis, autophagy and necrosis. Apoptosis, type I programmed cell death (PCD), plays an important role in chemotherapy-induced tumor cell death in variety of cancers[2]. Moreover, apoptosis activation in cancer therapy is irreversible and is commonly regarded as an efficient way to kill cancer cells. Apoptosis can be classified into two distinct signaling pathways: the extrinsic and intrinsic pathway [3]. In the extrinsic pathway, apoptosis is triggered by death receptors and activated by death receptor ligands (FASL, TNFα and TRAIL). On the other hand, the mitochondrial-initiated pathway (the intrinsic apoptosis) is usually associated with mitochondrial outer membrane permeabilization (MOMP) and the release of pro-apoptotic proteins such as Bax and activation of caspases [4].

Autophagy is a basic catabolic process, which is not only involved in energy homeostasis, cellular components turnover and development but also in cancer cell death. Autophagy is regarded as type-II PCD program that occurs in various cancer cells in response to anticancer therapies[5]. In some cellular settings, autophagy serves as a cell survival mechanism suppressing apoptosis, or in others it can lead to cell fate, either being together with apoptosis or being an alternative mechanism when the apoptosis is defective[6].

Reactive oxygen species（ROS） act as mediators of cell fate determined by the extent of oxidative damage, under physiological conditions, low levels of ROS result in

growth adaptation and survival[7]. In contrast, excessive ROS production induces cellular damage and promotes apoptotic, necrotic and autophagic cell death[8]. Cancer cells have a higher metabolic rate than normal cells, leading to comparatively higher intracellular ROS concentrations. Therefore, cancer cells are under increased oxidative stress, causing them to be more vulnerable to ROS-mediated insults induced by exogenous agents[9, 10]. It is well known that various ROS-inducing compounds are effective in cancer therapy by causing mitochondrial damage and cell death[11]. In addition, ROS are regulators of mitogen-activated protein kinase(MAPKs) signaling transduction, which mediates intracellular signal transduction in response to different physiological stimuli and stressing conditions[12]. C-Jun NH_2-terminal kinase (JNK) is one of the major MAPKs, JNK activation induce apoptosis. An increase in intracellular ROS, as well as activation of MAPKs plays a key role in many cellular events, including apoptosis and autophagy[13-15].

11-benzoyl-10-chloro-7,9-difluoro-6-imino-2,3,4,6-tetrahydro-1H-pyrimido[1,2-b]i soquinoline-8-carbonitrile (HC6h) compound is polyhalo 1,3-diazaheterocycle fused isoquinolin-1(2H)-imines derivative. It has been shown that isoquinolin-1(2H)-imine derivatives exhibit anti-malarial, anti-inflammatory, anti-tumor and antiviral properties[16]. We previously evaluated a series of polyhalo 1,3-diazaheterocycle fused issoquinolin-1(2H)-imines derivatives to ascertain the cytotoxicity in a series of cancer cell lines. We found that HC6h compound showed good anticancer activity in vitro and in vivo. Also, the HC6h compound inhibited S_{180} and H_{22} mice tumor growth and did not show any acute toxicity at the dosage of 5000mg/kg[16]. However, the underlying anti-tumor mechanism has not been identified before.

Here we investigated the mechanism of HC6h induced cell death in human adenocarcinoma lung cancer cells (A549). Exposure of A549 cells to HC6h resulted in cell death with morphological and biochemical changes characteristic of autophagy and apoptosis. Furthermore, we identified that the involvement of ROS production as well as JNK activation as upstream of HC6h-induced autophagic and apoptotic pathways. In addition, in combination with autophagy inhibitor, bafilomycin increased

4

the apoptotic effect of HC6h in A549 cells, suggesting that autophagic effect induced by HC6h acted as a cell repair mechanism to counteract the damaging effect caused by HC6h-induced ROS. Thus our results demonstrated the cytotoxic activity of HC6h by inducing both autophagy and apoptosis in A549 cells and its potential as a promising chemotherapeutic agent.

Materials and Methods

Chemicals

HC6h compound was synthesized according to the literature[17] at Key Laboratory of Medicinal Chemistry for Natural Resource (Yunnan University), Ministry Education, School of Chemical Science and Technology, Yunnan University, Kunming, P.R. China. In detail, a dry mortar was charged with HKAs 1 (1-phenyl-2-(tetrahydropyrimidin-2(1H)-ylidene) ethan-1-one, 1 mmol) and polyhaloisophthalonitrile 4 (5-chloro-2,4,6-trifluoroisophthalonitrile, 1.1 mmol). The mixture was mixed at room temperature by vigorously grinding with a pestle for a few minutes (1-2 min). The mixture was placed in a microwave tube and irradiated in a microwave reactor (Discover), with control of power and temperature by infrared detection, at 120℃ for 12 min (maximum power 200 W). After it was cooled, the resulting mixture was transferred to a 50 mL flask, and dissolved in 25 mL of dioxane, and addition of t-BuOK (1.5 mmol). Stirring at room temperature, the reaction process was monitored by TLC. After completion, the reaction mixture was poured into 60 mL of water and filtered to obtain the crude products, which were purified by column chromatography (petrol/ethyl acetate) 1:3, v/v) on silica-gel to give the desired product HC6h. The structure of HC6h that was used in our study is shown in Fig.1. Compounds were prepared as 100 mM stock solutions in DMSO and aliquots stored at -20 ℃, protected from light. Reagents, unless specified otherwise, originated from Sigma-Aldrich Ltd (China).

Cell lines and culture conditions

Human colon cancer cell lines (HCT116, HT29), human ovarian cancer (SK-OV-3), human breast cancer (MCF-7), human glioblastoma (U251), human lung cancer (A549)and normal lung fibroblast (MRC-5) cell lines were obtained from the American Type Culture Collection(Manassas, VA); HCT116, HT29, SK-OV-3 and A549 cells were grown in RPMI1640 medium (Hyclone, Thermo Scientific) supplemented with 10% fetal bovine serum (FBS), MRC-5, U251and MCF-7 cells were maintained in Dulbecco's modified Eagle's medium (DMEM) (Hyclone, Thermo Scientific) supplemented with 10% FBS. All cells were incubated at 37 °C under 5% CO_2. All cell lines were verified as mycoplasma free.

Growth Inhibitory Assays

Growth inhibition of human cancer cells by the synthetic polyhalo 1,3-diazaheterocycle fused iaoquinolin-1(2H)-imines derivative was assessed by the MTT assay, along with DMSO as a control. Different human cancer cell lines were treated with compound at various concentrations (0μM, 0.1μM, 1μM, 10μM, 50μM, 100μM). After a 72 h incubation, MTT [3-(4,5-dimethylthiazol-2-yl)-2,5-diphenyltetrazolium bromide] was added to the wells (50 μl; 0.4 mg/ml) and incubated another 4h. Medium were aspirated and DMSO (150 μl) was added to each well. Absorbance was measured at 490 nm using 2030 Multi-label Reader (Perkin-Elmer Victor X5, US). Compound concentrations causing 50% growth inhibition (IC_{50}) were calculated.

Measurement of intracellular ROS

Cellular ROS content was determined using the oxidation-sensitive fluorescent probe dye, 2',7'-dichlorofluorescein diacetate (H_2DCFDA) according to the manufacturer's instructions. Briefly, cells were collected and washed once with PBS and labeled for 30 min at 37C in the dark with 10 μM H_2DCFDA probe. The cells were then washed three times with PBS, and ROS levels (fluorescence intensity) were determined by

flow cytometry.

Mitochondrial Membrane Potential Assay

Mitochondrial membrane potential was measured by flow cytometry using the lipophilic cation 5,5',6,6'-tetrachloro-1,1',3,3'-tetraethylbenzimidazolyl-carbocyanine iodide (JC-1;). In healthy cells, JC-1 stains the mitochondria red whereas in cells with decreased mitochondrial membrane potential, JC-1 remains in the cytoplasm and emits green fluorescence. A549 cells treated at indicated concentrations and times were harvested and incubated with JC-1 at a final concentration of 1μg/mL for 30 min at 37℃. After staining, cells were washed twice with ice-cold PBS and subjected to flow cytometry analysis.

Western blot analysis

Treated cells were pelleted and lysed in the lysis buffer (2.5 mM EDTA, 2.5 mM EGTA, 20 mMNaF, 1 mM Na_3VO4, 100 Mm NaCl, 0.5% triton X-100) and freshly added protease inhibitor. Protein concentration was determined by Bradford assay. Cellular protein (50 μg) were separated by SDS polyacrylamide gel electrophoresis and blotted onto PVDF membranes. Membranes were blocked and probed overnight with the respective primary antibodies (LC3, p53, p-p53, PUMA, Bax, Bcl-2, caspase-3, caspase-9, PARP, JNK, p-JNK, p62, VDAC and tubulin,) (Cell Signaling Technology) followed by horseradish-peroxidase-coupled secondary antibodies. Chemiluminescence was performed with ECL kit (Thermo).

Cytochrome C release assay

A549 cells treated with vehicle and HC6h compound for 24 h were harvested and washed once with ice-cold PBS. The cells were then incubated with extraction buffer (Mitochondria/Cytosol Fractionation Kit, Abcam) on ice for 10 min. The supernatant containing the cytosol proteins and precipitations containing mitochondria were used for western blot analysis.

Annexin-V/PI assay

The Annexin-V/PI assay was performed with flow cytometry (BD, FACS Vantage SE) using the FITC-labeled Annexin-V and PI kit (Santa Cruz) according to the manufacturer's instructions. Briefly, cells were pelleted following HC6h treatment at indicated time, washed in PBS and resuspended in 100 μl of binding buffer containing annexin V-FITC and propidium iodide. Another 400 μl of binding buffer were added to the cells before flow cytometric analysis.

Quantification of acidic vesicular organelles with acridine orange

A549 cells were seeded into 6-well plates and allowed to attach overnight before treatment with 24 μM HC6h and vehicle. Cells were stained with acridine orange (final concentration 1 μg/ml) for 15 min. Media were removed and cells washed with PBS, trypsinized, re-suspended in PBS and analyzed by flow cytometry; green (510-530 nm, FL1-H channel) and red (> 650 nm, FL3-H channel). The bar for FL3-H in the control sample was set so that the acidic vesicular organelle (AVO) positive cells represented approximately 5% of the population. Compound-treated samples were measured under the same conditions.

Detection of punctuate GFP-LC3 punctate

GFP-LC3 was kindly provided by Dr EngHui Chew (National University of Singapore). A549 cells were seeded onto cover slips in 6-well plates at a density of 1×10^5 cells/well and left overnight. Cells were treated with 2, 6 12 and 24μM HC6h and vehicle, then transfected with 4 μg GFP-LC3 plasmid using LipofectAMINE2000 (Invitrogen Corporation)) according to manufacturer's instructions. After 72 h cells were fixed with 4% paraformaldehyde in PBS at 4 ℃ for 30 min, and GFP-LC3 fluorescence was examined under a fluorescence microscope. For each slide, 100 cells were analyzed and mean numbers of punctate GFP-LC3 spots/cell were calculated.

Small interfering RNA (siRNA) transfection

A549 cells were seeded into 6-well plate at a density of 1×10^6 cells /well and allowed to reach approximately 70% confluence on the day of transfection. The siRNA constructs used were obtained as siRNA control and siRNA against JNK (Genechem Biotech, China). Cells were transfected with 100nM siRNA using electroporation method (Amaxa, 10700634 AAD-1001, Germany) according to manufacturer's instruction. At 24h after transfection, the cells were treated with compound HC6h for 24h and examined by western blot.

Statistical analysis

The results were expressed as mean ±standard deviation (SD). Statistical differences were evaluated using the two-tailed Student's t-test and analysis of variance (ANOVA) followed by *q*- test, considered significant at $^*p < 0.05$, $^{**}p < 0.01$ or $^{***}p < 0.001$.

Results

HC6h decreases cell viability in human cancer cells

To assess the effect of HC6h on the inhibition of cell growth, A549, HCT116, HT29, MCF-7, SK-OV-3，U251 and MRC5 cells were exposed to various concentrations of HC6h compound for 72 h. As shown in table 1, the IC_{50} values of HC6h were 7.64μM for A549 cells, 13.87μM for HCT116, 13.65μM for HT29, 14.38μM for MCF-7, 17.06 μM for SK-OV-3, 15.02μM for U251 and 21.56μM for MRC-5 cells. As HC6h showed relatively good anticancer activity in A549 cells, we therefore investigated the mechanism of anticancer effect of HC6h in A549 cells.

HC6h rapidly induces the accumulation of intracellular ROS

It is reported that ROS can induce autophagy as well as apoptosis [15, 18]. Therefore, ROS generation was analyzed in HC6h-treated A549 cells by performing 2',7'-dichlorodihydrofluorescein diacetate(H_2DCFDA) staining followed by flow cytometry, H_2O_2 was included as a positive control. As shown in Figure2A, HC6h induced ROS generation in a time dependent manner, as reflected by the increase of

9

fluorescence intensity. The highest amount of ROS was generated after 6 h treatment of 24 μM HC6h compound in A549 cells. In addition, the enhanced ROS levels were significantly attenuated by treatment with N-acetylcysteine (NAC). Moreover, combination of NAC and HC6h attenuated the apoptotic and autophagic effects, as shown by diminished caspase-9 and caspase-3 activation, PARP cleavage, p53 and PUMA enhancement, also a decrease in LC3-II levels (Figure2B).

HC6h induced apoptosis in A549 cells

The apoptotic effect of HC6h treatment in A549 cells was explored. Mitochondria are known to play a pivotal role to apoptosis in response to many stresses and the loss of mitochondrial membrane potential (MMP) is a sensitive marker of early mitochondrial damage during apoptosis. We therefore used JC1 staining assay to investigate the mitochondrial membrane potential. HC6h treatment of A549 cells for 3h results in 12.5% decrease in mitochondrial membrane potential. 17.8% decrease was observed at 6h and 67.8% decrease in mitochondria membrane potential was observed at 12h (Figure 3A). Thus, mitochondrial membrane potential was significantly decreased after HC6h treatment in A549 cells, which indicated that accumulation of damaged mitochondria. Cytochrome C localized in the mitochondrial inner membrane and release into the cytosol upon apoptosis induction, exposure of A549 cells to HC6h induced the release of cytochrome C from mitochondria to the cytosol (Figure 3B). Bcl-2 family includes Bcl-2 and Bcl-2 related membranes such as Bax plays a crucial role in regulation of apoptosis. HC6h treatment can significantly reduce the expression level of anti-apoptotic Bcl-2 while induce the level of pro-apoptotic Bax in a dose dependent manner, leading to an increase in Bax/Bcl-2 ratio (3.26 fold *vs.* control), which is in favor for apoptosis induction (Figure3C).

Bcl-2 family members located in the mitochondrial membranes and trigger the activation of caspase[19].To gain further insight into the mechanism by which HC6h induced cell death, we examined the effect of HC6h treatment on the apoptosis of A549 cells. Flow cytometry analysis via Annexin V/PI staining was performed to

investigate the pro-apoptotic effect on A549 cells. It was shown that HC6h treated cells undergo apoptosis at significantly higher rate than control cells with a concentration dependent manner (Figure 3D).

A549 cells activated incomplete autophagy with HC6h treatment

Light microscopy observation of HC6h (24μM, 48 h) treated A549 cells revealed several morphological changes, such as cytoplasmic vacuolation and cell shrinkage (Figure 4A). These vacuoles might arise due to the cell autophagy. We therefore postulated that autophagy would be triggered in A549 cells on HC6h treatment. Formation of acidic vesicular organelles (AVOs) was observed in HC6h-treated cells in time dependent manner when stained with the lysosome-tropic agent acridine orange by FACS analysis, and formation of AVO was markedly suppressed in the presence of 3-methyladenine (3-MA), an early stage of autophagosome inhibitor (Figure 4B). LC3 is an autophagy marker which exists in two forms, an 18-KDa cytosolic protein (LC3-I) and a processed 16-kDa form (LC3-II) that is membrane-bound and increased during autophagy by conversion from LC3-I [20]. Therefore, we examined LC3 distribution in response to HC6h treatment in A549 cells. As shown in Figure 4C, in control cells, GFP-LC3 was weakly expressed in the cytoplasm, whereas, HC6h treatment remarkably increased punctuate structure of GFP-LC3, also the percentage of puncta of GFP-LC3 was enhanced with the increasing concentration of HC6h. Furthermore, induction of autophagy was further supported by the conversion of light chain 3 LC3-1 to LC3-II in a concentration dependent manner upon HC6h treatment (Figure 4D). To further identify whether the autophagy induced by HC6h treatment was complete, we analyzed the expression of LC3 and p62 by using autophagosome inhibitor 3-MA and CQ. Our data showed that the expression level of autophagy substrate p62 had a little increasing and the phenomenon was more significant after 3-MA or CQ treatment together. These results suggest the induction of an incomplete after HC6h treatment.

Inhibition of autophagy by HC6h induced apoptosis

Cell death could be augmented when autophagy is suppressed, suggesting a pro-survival role of autophagy. To assess the role of autophagy in HC6h induced cancer cell death, autophagy inhibitor bafilomycin A1was used in combination with HC6h in A549 cells, apoptosis induction was examined in A549 cells by flow cytometry following annexin-V/PI staining of cells exposed to HC6h in the presence or absence of bafilomycin. Treatment with HC6h alone (24μM) induced apoptosis in A549 cells with an early apoptotic percentage of 14.3%. Bafilomycin(100nM) *per se* did not have any effect on apoptosis in A549 cells; combination of HC6h with bafilomycin increased significant apoptosis (23.0%) compared with HC6h alone treatment (14.3%)(Figure 5A). Characteristic morphological changes associated with apoptosis induction were observed after simultaneous incubation with bafilomycin and HC6h: cells rounded up, appeared smaller and detached from the plates (data not shown). Moreover, cleavage of PARP, caspase-9 and caspase-3 was observed at low concentration of HC6h (2μM) in combination with bafilomycin, compared with HC6h alone treatment (12 μM) (Figure 5B). These data indicate that A549 cells underwent increased apoptosis when exposure to HC6h compound combined with autophagy inhibitor bafilomycin. The inhibition of HC6h-induced autophagy accelerated HC6h induced apoptosis, these findings suggest that HC6h-induced autophagy may play some role as a survival mechanism against apoptosis.

Activation of JNK

JNK，a member of MAPK family, plays essential role in cell death. The JNK pathway is critical for the mediation of both autophagy and apoptosis. HC6h induced JNK phosphorylation (p-JNK) in a concentration-dependent manner. Notably, the inductions of p-JNK and p-53 were conferred by the increased ROS levels, as NAC inhibited JNK activation, suggesting that intracellular ROS acts supstream of JNK to mediate the actions of compound HC6h (Figure 6A). Furthermore, JNK serves as a critical mediator of HC6h-induced apoptosis as evidenced by the rescue of PARP and

caspase-3 cleavage and the LC3 conversion by JNK inhibitor SP600125 and siRNA-mediated depletion of JNK (Figure 6B and 6C). Taken together, these results indicate that the activation of JNK is required for HC6h-induced apoptosis in A549 cells.

Discussion

Chemotherapy remains the mainstream of tumor treatments, and the ultimate goal of successful chemotherapy is to induce robust apoptosis with simultaneous inhibition of survival signaling in cancer cells with minimal toxicity to normal cells. Autophagy as well as apoptosis is an emerging target as anticancer therapy. A variety of evidence has represented the complex interplay between apoptosis and autophagy and which can cooperate, antagonize or assist each other[6, 21]. In several studies, autophagy induction has been shown to enhance tumor cell survival, thereby counteracting or restricting the efficacy of apoptosis induction by chemotherapeutic agents[22]. One previous study reported that HC6h showed good anti-cancer effect in various cancer cell lines and also inhibited S_{180} and H_{22} mice tumor growth and did not show any acute toxicity at the dosage of 5000mg/kg[16]. In our study we found that HC6h compound possess good anticancer activity in A549 cancer cells (IC_{50}=7.64μM) compared with normal fibroblast MRC-5 cells (IC_{50}=21.56μM) (Table 1). It is well documented that cancer cells frequently have increased burden of oxidative stress and therefore are likely to be more sensitive to the damage promoted by further ROS insults[23]. Regardless of how ROS are generated, ROS rise has two potential consequences: damage to cellular components and triggering various signaling pathways[10, 24]. A wide arrange of evidence shows a link between ROS and autophagy and apoptosis[7, 25, 26]. Here we found that HC6h induces apoptosis and autophagy in cancer cells through the induction of oxidative stress. Treatment of cancer cells with HC6h in vitro leads to the rapid generation of ROS. Scavenging of ROS by antioxidant NAC completely reversed the HC6h-induced apoptosis and autophagy (Figure 2).

13

Apoptosis is a process essential for development and maintenance of tissue homeostasis, and also a major process to eradicate cancer cells. It is conceivable that PUMA (p53 upregulated modulator of apoptosis) plays an important role in p53-mediated apoptosis and its over-expression is associated with the translocation of Bax to the mitochondria that in turn result in the loss of MMP and subsequently the release of cytochrome C. The release of cytochrome C initiates the formation of apoptosome through interaction with Apaf-1 (apoptotic protease-activating factor) which is a key regulator of programmed cell death [4, 27]. We revealed that mitochondria dysfunction was observed after exposure of A549 cells to HC6h, which was displayed by some alterations at mitochondria-related events, such as loss of mitochondrial membrane potential, cytochrome c release and changes of Bax and Bcl-2 expressions (Figure 3). HC6h also leads to PUMA and p53 up-regulation, caspase-9, caspase-3 and PARP cleavage. Therefore efficient intrinsic apoptosis pathway is triggered by HC6h treatment in A549 cells.

In addition, we found that autophagy was induced by HC6h as evidenced by accumulation of AO-staining acidic vesicles, formation of autophagosomes observed with increased number of puncta LC3 and up-regulation of LC3-II. However, we found that the expression level of autophagy substrate p62 increased with concentration dependent. Furthermore, the increasing was more significant with 3-MA and CQ treatment. 3-MA is selective PI3K inhibitors which can inhibit the shift of LC3-1 to LC3-II and block the formation of autophagosome. Another small molecules CQ inhibits autophagy by destroying the lysosome function. Therefore, the autophagy induced by HC6h was an incomplete autophagy in A549 cells. It is well known that autophagy could limit the effects of cytotoxic anticancer agents through its ability to clear damaged organelles and proteins, which may help cancer cells to survive chemotherapy-induced stress. In these scenarios, suppressing autophagy could be beneficial to treatment outcome. We revealed that autophagy inhibitor bafilomycinA1 significantly augmented cell death on HC6h treatment in A549 cells (Figure 4).

Various apoptotic stimuli can rapidly activate MAPKs, which include JNK. So far,

14

increasing evidences indicated that JNK is primarily activated by various stresses including UV radiation, heat shock, oxidative stress, chemotherapeutic agents and protein synthesis inhibitors, especially, oxidative stress is important [28]. We found that A549 cells with HC6h treatment in vitro leads to the rapid generation of JNK phosphorylation. Furthermore, the JNK inhibitor SP600125 and ShRNA JNK significantly attenuate the promoting autophagy effects. In addition, JNK phosphorylation was potently abolished by NAC suggested that HC6h induced apoptosis and autophagy through ROS-dependent JNK pathway.

In conclusion, this study showed that isoquinolin-1(2*H*)-imine derivative HC6h compound inhibited the proliferation of A549, HCT116 and HT29 cells. HC6h induced apoptosis and autophagy via the ROS-dependent JNK signaling pathway in A549 cells. Cancer cells activated incomplete autophagy with HC6h treatment and inhibition of autophagy by autophagy inhibitor significantly augmented cell death on HC6h treatment (Figure 7). This compelling evidence suggested that HC6h might be a potential candidate for the development of new chemotherapy agents for the treatment of non-small cell lung cancer. However, the potential of this molecule in the treatment of other cancer is still unknown, further study need to be evaluated in other cancers.

15

References

1   Hanahan D, Weinberg RA: Hallmarks of cancer: the next generation. Cell 2011;144:646-674.

2   Zimmermann KC, Bonzon C, Green DR: The machinery of programmed cell death. Pharmacology & therapeutics 2001;92:57-70.

3   Johnstone RW, Ruefli AA, Lowe SW: Apoptosis. Cell;108:153-164.

4   Tait SW, Green DR: Mitochondria and cell death: outer membrane permeabilization and beyond. Nat Rev Mol Cell Biol 2010;11:621-632.

5   Yang Z, Klionsky DJ: Eaten alive: a history of macroautophagy. Nat Cell Biol 2010;12:814-822.

6   Eisenberg-Lerner A, Bialik S, Simon HU, Kimchi A: Life and death partners: apoptosis, autophagy and the cross-talk between them. Cell Death Differ 2009;16:966-975.

7   Zhang L, Wang K, Lei Y, Li Q, Nice EC, Huang C: Redox signaling: Potential arbitrator of autophagy and apoptosis in therapeutic response. Free Radic Biol Med 2015;89:452-465.

8   Li L, Ishdorj G, Gibson SB: Reactive oxygen species regulation of autophagy in cancer: Implications for cancer treatment. Free Radical Biology and Medicine 2012;53:1399-1410.

9   Pelicano H, Carney D, Huang P: ROS stress in cancer cells and therapeutic implications. Drug resistance updates : reviews and commentaries in antimicrobial and anticancer chemotherapy 2004;7:97-110.

10   Trachootham D, Alexandre J, Huang P: Targeting cancer cells by ROS-mediated mechanisms: a radical therapeutic approach? Nat Rev Drug Discov 2009;8:579-591.

11   Ling LU, Tan KB, Lin H, Chiu GN: The role of reactive oxygen species and autophagy in safingol-induced cell death. Cell death & disease 2011;2:e129.

12   Shen HM, Liu ZG: JNK signaling pathway is a key modulator in cell death

mediated by reactive oxygen and nitrogen species. Free radical biology & medicine 2006;40:928-939.

13   Kyriakis JM, Banerjee P, Nikolakaki E, Dai T, Rubie EA, Ahmad MF, Avruch J, Woodgett JR: The stress-activated protein kinase subfamily of c-Jun kinases. Nature 1994;369:156-160.

14   Avisetti DR, Babu KS, Kalivendi SV: Activation of p38/JNK pathway is responsible for embelin induced apoptosis in lung cancer cells: transitional role of reactive oxygen species. PloS one 2014;9:e87050.

15   Li HY, Zhang J, Sun LL, Li BH, Gao HL, Xie T, Zhang N, Ye ZM: Celastrol induces apoptosis and autophagy via the ROS/JNK signaling pathway in human osteosarcoma cells: an in vitro and in vivo study. Cell Death Dis 2015;6:e1604.

16   Huang C, Yan SJ, Zeng XH, Dai XY, Zhang Y, Qing C, Lin J: Biological evaluation of polyhalo 1,3-diazaheterocycle fused isoquinolin-1(2H)-imine derivatives. Eur J Med Chem 2011;46:1172-1180.

17   Yan S, Huang C, Su C, Ni Y, Lin J: Facile route to 1,3-diazaheterocycle-fused [1,2b]Isoquinolin-1(2H)-one derivatives via substitution-cyclization reactions. J Comb Chem 2010;12:91-94.

18   Lee IK, Kang KA, Lim CM, Kim KC, Kim HS, Kim DH, Kim BJ, Chang WY, Choi JH, Hyun JW: Compound K, a metabolite of ginseng saponin, induces mitochondria-dependent and caspase-dependent apoptosis via the generation of reactive oxygen species in human colon cancer cells. Int J Mol Sci 2010;11:4916-4931.

19   Adams JM, Cory S: The Bcl-2 protein family: arbiters of cell survival. Science 1998;281:1322-1326.

20   Mizushima N, Yoshimori T, Levine B: Methods in mammalian autophagy research. Cell 2010;140:313-326.

21   Radogna F, Dicato M, Diederich M: Cancer-type-specific crosstalk between autophagy, necroptosis and apoptosis as a pharmacological target. Biochemical Pharmacology 2015;94:1-11.

22 Bao L, Jaramillo MC, Zhang Z, Zheng Y, Yao M, Zhang DD, Yi X: Induction of autophagy contributes to cisplatin resistance in human ovarian cancer cells. Mol Med Rep 2015;11:91-98.

23 Huang P, Feng L, Oldham EA, Keating MJ, Plunkett W: Superoxide dismutase as a target for the selective killing of cancer cells. Nature 2000;407:390-395.

24 Yang YJ, Baek JY, Goo J, Shin Y, Park JK, Jang JY, Wang SB, Jeong W, Lee HJ, Um HD, Lee SK, Choi Y, Rhee SG, Chang TS: Effective Killing of Cancer Cells Through ROS-Mediated Mechanisms by AMRI-59 Targeting Peroxiredoxin I. Antioxid Redox Signal 2015

25 Navarro-Yepes J, Burns M, Anandhan A, Khalimonchuk O, del Razo LM, Quintanilla-Vega B, Pappa A, Panayiotidis MI, Franco R: Oxidative stress, redox signaling, and autophagy: cell death versus survival. Antioxid Redox Signal 2014;21:66-85.

26 Cao J, Ying M, Xie N, Lin G, Dong R, Zhang J, Yan H, Yang X, He Q, Yang B: The oxidation states of DJ-1 dictate the cell fate in response to oxidative stress triggered by 4-hpr: autophagy or apoptosis? Antioxid Redox Signal 2014;21:1443-1459.

27 Danial NN, Korsmeyer SJ: Cell death: critical control points. Cell 2004;116:205-219.

28 Dhanasekaran DN, Reddy EP: JNK signaling in apoptosis. Oncogene 2008;27:6245-6251.

Figure Legends

Figure 1 chemical structure of HC6h

Figure 2 Induction of ROS accumulations in A549 cells. (A) Effect of HC6h on ROS production. (B) Effects of HC6h and NAC on the expressions of apoptotic protein.

Figure 3 Induction of apoptosis in A549 cells. (A)Loss of mitochondria membrane potential was induced by HC6h treatment. (B) HC6h induced cytochrome c release. (C) HC6h induced the ratio of Bax/Bcl-2 increased (D) Induction of apoptosis was analyzed by flow cytometry.

Figure 4 A549 cells activated incomplete autophagy with HC6h treatment. (A) Cell morphological change and double membrane vesicles were formed after HC6h compound treatments. (B) Formation of AVOs (acidic vesicular organelles) was determined in A549 cells treated with HC6h. (C) GFP-LC3 punctan induced by HC6h over concentration course (D) Expression level of p62 and LC3-II with 3-MA and CQ treatment.

Figure 5 Effects of autophagy inhibitor bafilomycin on apoptosis induced by HC6h. (A) Apoptotic effects in combination with bafilomycin were analyzed by flow cytometry with Annexin V/PI staining. (B) Apoptotic protein expressions in combination with bafilomycin.

Figure 6 ROS generation induced by HC6h is necessary for activation JNK. (A) Effects of NAC on the JNK and p-p53 activation in A549 cells. (B) Effects of apoptosis and autophagy with JNK inhibitor SP600125. (C) Effects of apoptosis and autophagy with silencing of JNK by siRNAs.

Figure 7 Proposed models representing the mechanism of action of HC6h in A549 cells.
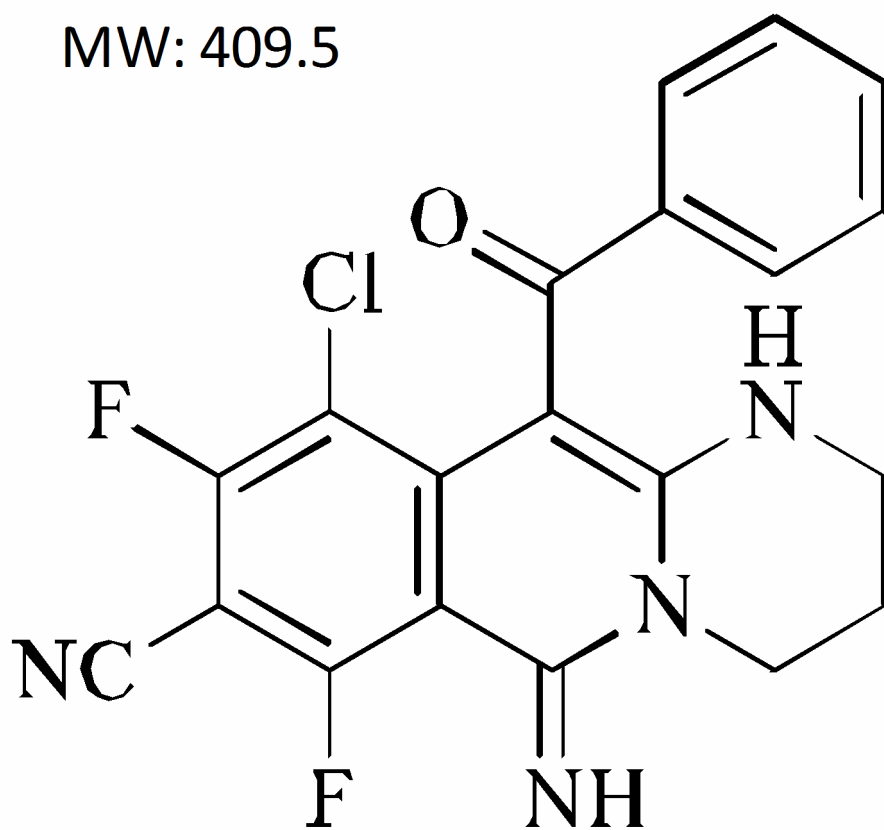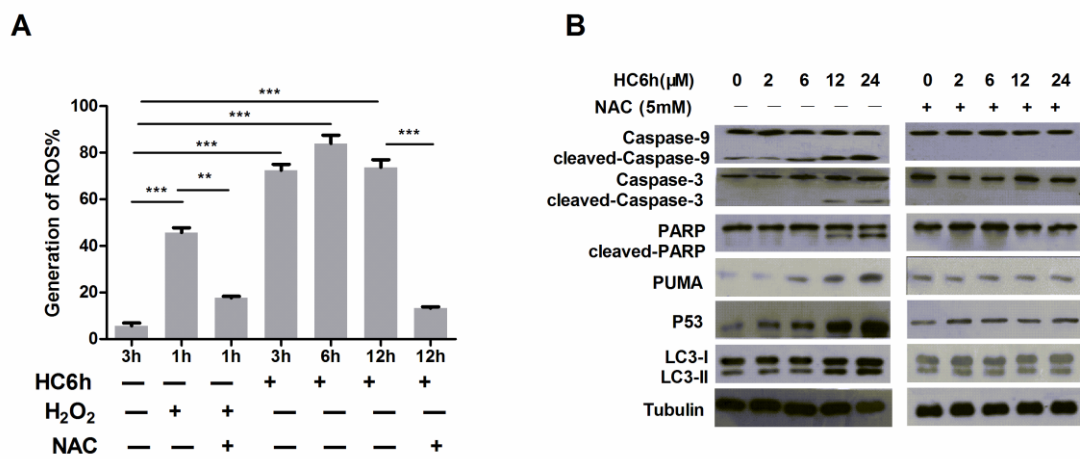
MW: 409.5

Figure 1
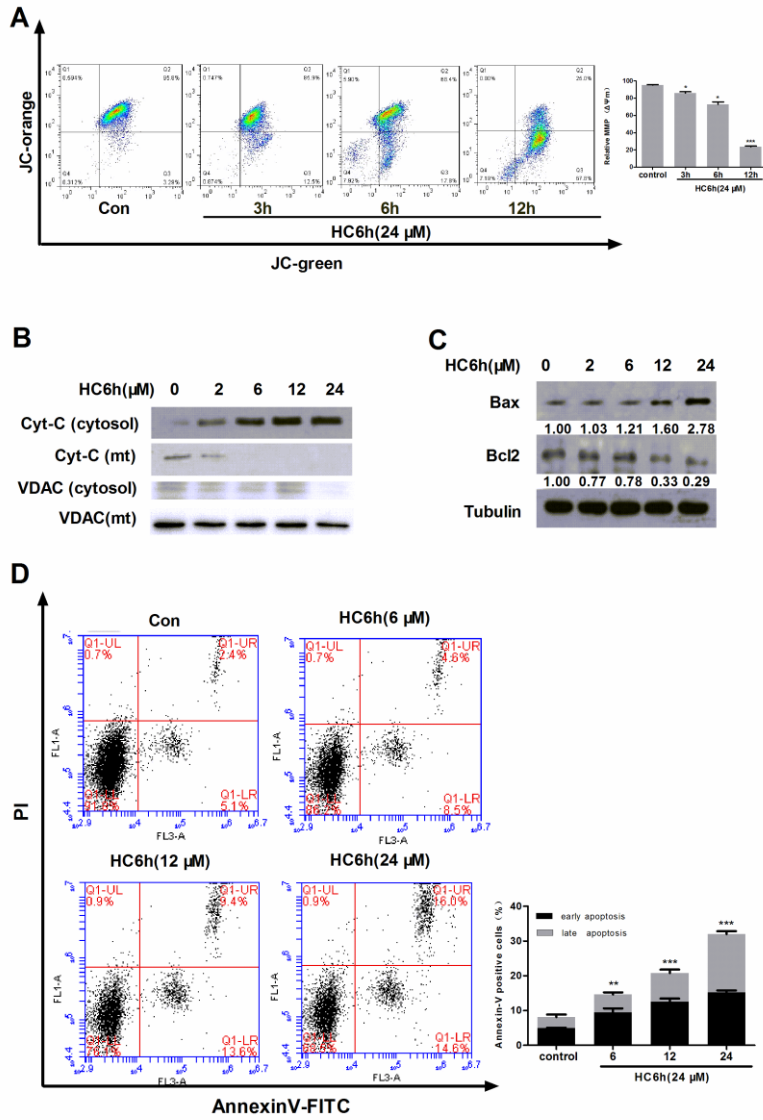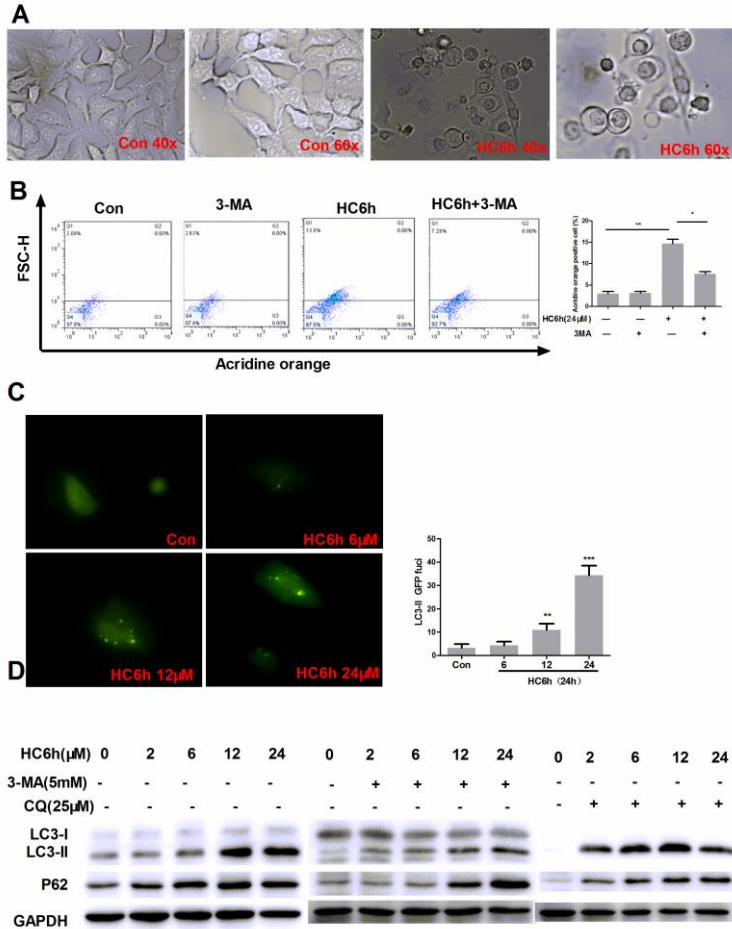
Figure 2

Figure 3

Figure 4
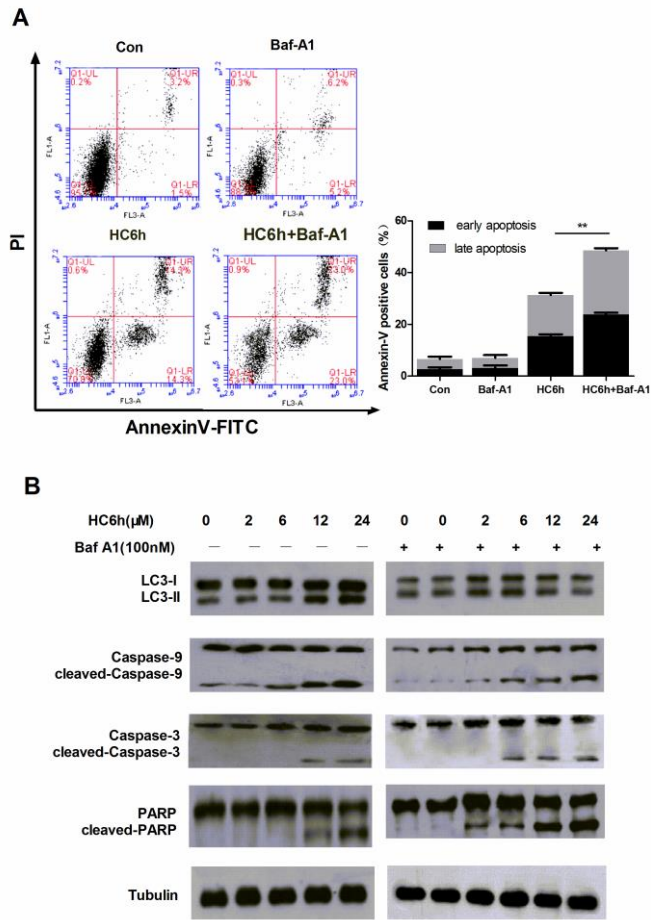
Figure 5
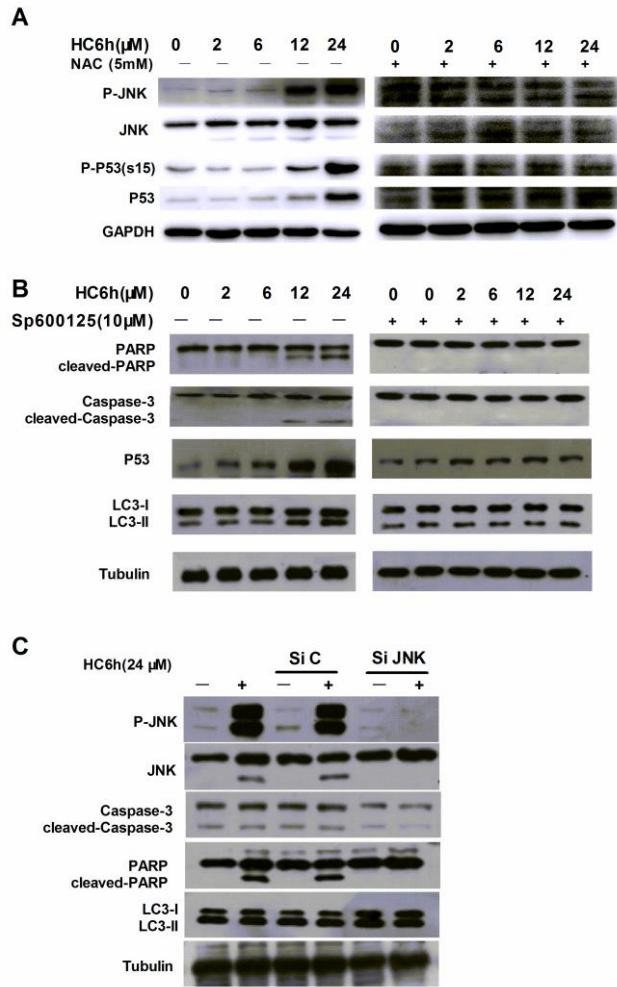
Figure 6
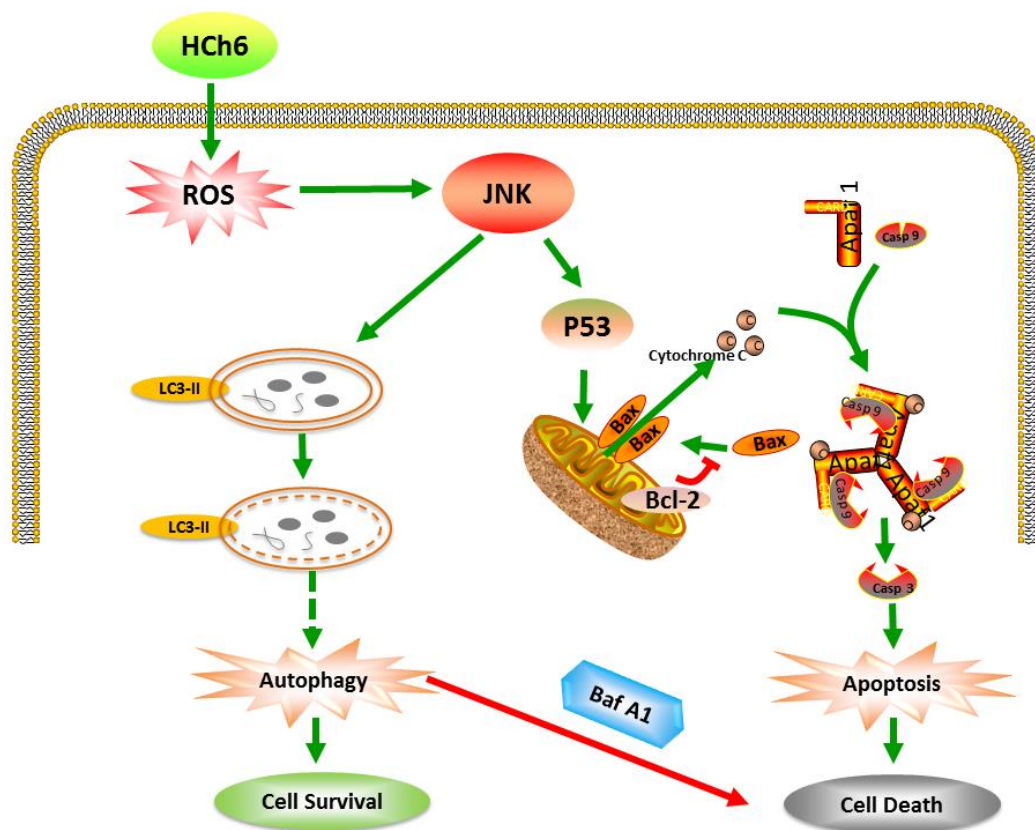
Figure 7

Table 1 IC$_{50}$ values of HC6h on the growth inhibition of cancer cells

Compound	Cell lines IC$_{50}$（μM）						
	MRC5	A549	HCT116	HT29	MCF-7	SK-OV-3	U251
HC6h	21.56±0.51	7.64±0.38	13.87±1.60	13.65±0.59	14.38±1.52	17.06±1.63	15.02±0.13

The growth inhibitory activity, determined as IC$_{50}$ values for each cell line by 72 h MTT assay. Data represent the mean values of three independent experiments.